

High-Efficiency White Organic Light-Emitting Devices Based on a Highly Amorphous Iridium(III) Orange Phosphor

Xiao-Ming Yu,[†] Hoi-Sing Kwok,^{*,†} Wai-Yeung Wong,^{*,‡} and Gui-Jiang Zhou[‡]

Department of Electrical and Electronic Engineering and Center for Display Research, Hong Kong University of Science and Technology, Clear Water Bay, Hong Kong, and Department of Chemistry and Centre for Advanced Luminescence Materials, Hong Kong Baptist University, Waterloo Road, Hong Kong

Received May 4, 2006. Revised Manuscript Received August 14, 2006

An efficient multilayer white organic light-emitting diode (WOLED) based on a new orange phosphorescent iridium complex [Ir(L)₃] (HL = (9,9-diethyl-7-pyridinylfluoren-2-yl)diphenylamine) was fabricated. The WOLED device employs two emission layers in which one layer contains 5% [Ir(L)₃] doped in the CBP host matrix (CBP = 4,4'-N,N'-dicarbazolebiphenyl) and another layer is composed of the mCP host (mCP = N,N'-dicarbazolyl-3,5-benzene) doped with a 8% blue-emitting phosphor, iridium(III)bis(4,6-di-fluorophenyl)-pyridinato-N,C²)picolinate (FIrPic). The threshold voltage of the device is 4.2 V, and the brightness reaches 3200 cd/m² at 10 V and 30 mA/cm². The color of the white light corresponds to the Commission Internationale de L'Eclairage (CIE) coordinates of (0.31, 0.41) and a strong voltage dependence of the electroluminescence spectrum is observed, with the blue color intensity increasing relative to the orange component at increasing voltage. The maximum current efficiency of 17.8 cd/A and power efficiency of 7.6 lm/W are achieved for the WOLED device.

Introduction

White organic light-emitting diodes (WOLEDs) have drawn much recent attention in the scientific and industrial sectors because of their potential use in display backlights, full color display applications, and solid-state lighting purposes.^{1,2} The combination of white emission and color filters should simplify the fabrication process of fine-pixel large-screen displays.³ WOLEDs can make attractive candidates as future illumination sources over the conventional incandescent bulbs and fluorescent lamps for several reasons, including compact size, the suitability for fabrication on flexible substrates, low operating voltages, and good power efficiencies.⁴ In particular, WOLEDs employing phosphorescent materials have led to significant improvements in efficiency, targeting backlights for full-color active-matrix displays combined with color filters.^{4–6} A number of device structural concepts have been employed to generate white electrophosphorescence. These include the doping of ap-

propriate amount of red (R), green (G), and blue (B) dopants in the same host in a single layer,^{7,8} the microcavity effect of one emission layer,⁹ use of exciplex formation,^{10,11} etc. Among these, the most common approach in WOLEDs is to use three separate emitters, each emitting one primary color from R, G, and B. Efficient WOLEDs have been prepared using this stacked concept with both fluorescent^{12,13} and phosphorescent emitters.¹⁴ Alternatively, more simplified architectures have also been described, which use dual-component fluorescent blue and orange emitters doped into separate layers.^{15–17} Here, an orange emitter can be consid-

* To whom correspondence should be addressed. Fax: +852-34117348. Tel.: +852-34117074. E-mail: rwywong@hkbu.edu.hk.

[†] Hong Kong University of Science and Technology.

[‡] Hong Kong Baptist University.

- (1) Friend, R. H.; Gymer, R. W.; Holmes, A. B.; Burroughes, J. H.; Marks, R. N.; Taliani, C.; Bradley, D. D. C.; Dos Santos, D. A.; Brédas, J. L.; Lögdlund, M.; Salaneck, W. R. *Nature (London)* **1999**, *397*, 121.
- (2) Heeger, A. J. *Solid State Commun.* **2001**, *73*, 681.
- (3) Li, J. Y.; Liu, D.; Ma, C.; Lengyel, O.; Lee, C.-S.; Tung, C. H.; Lee, S. T. *Adv. Mater.* **2004**, *16*, 1538.
- (4) (a) Justel, T.; Nikol, H.; Ronda, C. *Angew. Chem., Int. Ed.* **1998**, *37*, 3084. (b) Tokito, S.; Iijima, T.; Tsuzuki, T.; Sato, F. *Appl. Phys. Lett.* **2003**, *83*, 2459.
- (5) Sun, Y.; Giebink, N. C.; Kanno, H.; Ma, B.; Thompson, M. E.; Forrest, S. R. *Nature (London)* **2006**, *440*, 908.
- (6) Mameno, K.; Nishikawa, R.; Suzuki, K.; Matsumoto, S.; Yamaguchi, T.; Yoneda, K.; Hamada, Y.; Kanno, H.; Nishio, Y.; Matsuoka, H.; Saito, Y.; Oima, S.; Mori, N.; Rajeswaran, G.; Mizukoshi, S.; K. Hatwar, T. *IDW'02 Proceedings* **2002**, 235.

- (7) D'Andrade, B. W.; Holmes, R. J.; Forrest, S. R. *Adv. Mater.* **2004**, *16*, 624.
- (8) (a) Kido, J.; Shionoya, H.; Nagai, K. *Appl. Phys. Lett.* **1995**, *67*, 2281. (b) Ko, Y. W.; Chung, C.-H.; Lee, J. H.; Kim, Y.-H.; Sohn, C.-Y.; Kim, B.-C.; Hwang, C.-S.; Song, Y.-H.; Lim, J.; Ahn, Y.-J.; Kang, G.-W.; Lee, N.; Lee, C. *Thin Solid Films* **2003**, *426*, 246. (c) Che, C.-M.; Chan, S.-C.; Xiang, H.-F.; Chan, M. C. W.; Liu, Y.; Wang, Y. *Chem. Commun.* **2004**, 1484. (d) Liu, J.; Zhou, Q.; Cheng, Y.; Geng, Y.; Wang, L.; Ma, D.; Jing, X.; Wang, F. *Adv. Funct. Mater.* **2006**, *16*, 957. (e) Gong, X.; Wang, S.; Moses, D.; Bazan, G. C.; Heeger, A. J. *Adv. Mater.* **2005**, *17*, 2053. (f) Chuen, C. H.; Tao, Y. T. *Appl. Phys. Lett.* **2002**, *81*, 4499. (g) Gong, X.; Ma, W.; Ostrowski, J. C.; Bazan, G. C.; Moses, D.; Heeger, A. J. *Adv. Mater.* **2004**, *16*, 615.
- (9) (a) Kanno, H.; Sun, Y.; Forrest, S. R. *Appl. Phys. Lett.* **2005**, *86*, 263502. (b) Dodabalapur, A.; Rothberg, L. H.; Miller, T. M. *Appl. Phys. Lett.* **1994**, *65*, 2308.
- (10) Thompson, J.; Blyth, R. I. R.; Mazzeo, M.; Anni, M.; Gigli, G.; Cingolani, R. *Appl. Phys. Lett.* **2001**, *79*, 560.
- (11) (a) Adamovich, V.; Brooks, J.; Tamayo, A.; Alexander, A. M.; Djurovich, P. I.; D'Andrade, B. W.; Adachi, C.; Forrest, S. R.; Thompson, M. E. *New J. Chem.* **2002**, *26*, 1171. (b) D'Andrade, B. W.; Brooks, J.; Adamovich, V.; Thompson, M. E.; Forrest, S. R. *Adv. Mater.* **2002**, *14*, 1032.
- (12) Huang, Y. S.; Jou, J. H.; Weng, W. K.; Liu, J. M. *Appl. Phys. Lett.* **2002**, *80*, 2782.
- (13) Kido, J.; Kimura, M.; Nagai, K. *Science* **1995**, *267*, 1332.
- (14) (a) D'Andrade, B. W.; Thompson, M. E.; Forrest, S. R. *Adv. Mater.* **2002**, *14*, 147. (b) Tanaka, I.; Suzuki, M.; Tokito, S. *Jpn. J. Appl. Phys.* **2003**, *42*, 2737. (c) Ko, C. W.; Tao, Y. T. *Appl. Phys. Lett.* **2001**, *79*, 4234.

ered as a mixture of R and G and a combination of the two colors in appropriate ratio is expected to make a white light device. Also, a previous study has shown that the hole-transporting layer (HTL) which is doped with both a yellow and a red emitters can be combined with the blue emitter to achieve a white light emission.¹⁸ More recently, in addressing the challenge of making a solution-processed device, a number of reports have appeared based on the use of a single copolymer (both organic and organometallic) in the realization of highly efficient polymer WOLEDs.¹⁹

To obtain high-purity white light corresponding to the ideal CIE coordinates of (0.33, 0.33), careful matching of the emission colors and the concentration of each dye is required to achieve a well-balanced emission color. For blue dopants, it is common to use 4,4'-bis(9-ethyl-3-carbazolylvinylene)-1,1'-biphenyl (BCzVBi) or 4,4'-bis(2,2'-diphenylvinyl)-1,1'-biphenyl (DPVBi) as the fluorescent material, and iridium(III)bis(4,6-di-fluorophenyl)-pyridinato-*N,C*²picolinate (FIrPic) as the phosphor dye. For orange light, rubrene (tetraphenyl-naphthacene) is the most popular one. However, one of the best WOLEDs reported so far using the fluorescent rubrene only attained a current efficiency of 11 cd/A.^{16a} In order to get high-efficiency WOLEDs, we have to resort to orange-emitting metal phosphors.^{4–6,20} While electrophosphorescent OLEDs have been shown to have very high external quantum efficiency when used for monochromatic light emission,²¹ their incorporation into a white light-emitting device should

lead to similarly high-efficiency devices. Among phosphorescent heavy-metal compounds reported, cyclometalated iridium(III) complexes have emerged as the most promising materials for high-performance work because they show intense triplet emission at room temperature and significantly shorter phosphor lifetime when compared with other heavy-metal compounds.²¹ The device efficiency and emission color of iridium-based OLEDs can be modified easily by tuning the structure of the organic ligand chromophore.²¹

In this paper, a novel iridium(III) cyclometalated complex [Ir(L)₃] (**1**, HL = (9,9-diethyl-7-pyridinylfluoren-2-yl)diphenylamine) containing a diphenylaminofluorene framework which emits very strong orange color both in steady-state emission and electrophosphorescence can be exploited in the realization of WOLEDs. We have successfully fabricated a highly efficient dual emission layer WOLED based on this orange phosphor in combination with the blue phosphor iridium(III)bis(4,6-di-fluorophenyl)-pyridinato-*N,C*²picolinate (FIrPic) to produce a white light source with CIE coordinates of (0.31, 0.41). The highest luminous efficiency of the WOLED device can reach 17.8 cd/A.

Experimental Section

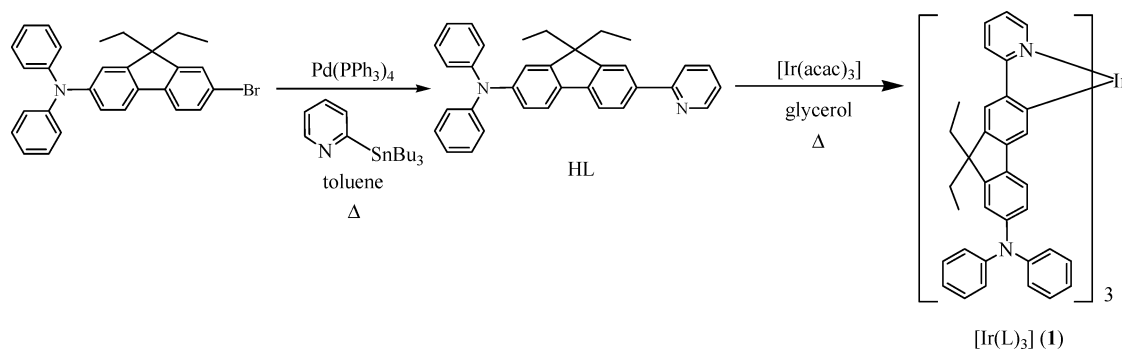
General. All reactions were performed under a nitrogen atmosphere with the use of standard Schlenk techniques. Solvents were carefully dried and distilled from appropriate drying agents prior to use (sodium benzophenone-ketyl for hexane and toluene, CaH₂ for CH₂Cl₂). Commercially available reagents were used without further purification unless otherwise stated. The procedure for the synthesis of (7-bromo-9,9-diethylfluoren-2-yl)diphenylamine followed the methods reported in the literature.²² All reactions were monitored by thin-layer chromatography (TLC) with Merck pre-coated glass plates. Flash column chromatography was carried out using silica gel from Merck (230–400 mesh). Fast atom bombardment (FAB) mass spectra were recorded on a Finnigan MAT SSQ710 system. NMR spectra were measured in CDCl₃ on a Varian Inova 400 MHz FT-NMR spectrometer; chemical shifts were quoted relative to the internal standard tetramethylsilane for ¹H and ¹³C-¹H NMR data. UV–vis spectra were obtained on a HP-8453 spectrophotometer. The photoluminescent properties and lifetimes of the compounds were probed on the Photon Technology International (PTI) Fluorescence Master Series QM1 system. The phosphorescence quantum yields were determined in CH₂Cl₂ solutions at 293 K against fac-[Ir(ppy)₃] as a reference ($\Phi_P = 0.40$).²³ For solid-state emission spectral measurements, the 325 nm line of a He-Cd laser was used as an excitation source. The luminescence spectra were analyzed by a 0.25 m focal length double monochromator with a Peltier cooled photomultiplier tube and processed with a lock-in amplifier. Electrochemical measurements were made using a BAS CV-50W model potentiostat. A conventional three-electrode configuration consisting of a platinum working electrode, a Pt-wire counter electrode, and an Ag/AgCl reference electrode was used. The solvent in all measurements was THF, and the supporting electrolyte was 0.1 M [Bu₄N]PF₆. Ferrocene was added as a calibrant after each set of measurements, and all potentials reported were quoted with reference to the ferrocene–ferrocenium (Fc/Fc⁺) couple at a scan rate of 100 mV s⁻¹. Thermal

- (15) Yang, J.; Jin, Y.; Heremans, P.; Hoefnagels, R.; Dieltiens, P.; Blockhuys, F.; Geise, H.; Van der Auweraer, M.; Borghs, G. *Chem. Phys. Lett.* **2000**, *325*, 251.
- (16) (a) Li, G.; Shinar, J. *Appl. Phys. Lett.* **2003**, *83*, 5359. (b) Zhang, Y.; Cheng, G.; Zhao, Y.; Hou, J.; Liu, S. *Appl. Phys. Lett.* **2005**, *86*, 011112-1.
- (17) Wang, L.; Duan, L.; Lei, G.; Qiu, Y. *Jpn. J. Appl. Phys.* **2004**, *43*, L560.
- (18) Hatwar, T. K.; Young, P. H.; Brown, C. T. U.S. Patent 6875524, Apr. 5, 2005.
- (19) (a) Liu, J.; Zhou, Q.; Cheng, Y.; Geng, Y.; Wang, L.; Ma, D.; Jing, X.; Wang, F. *Adv. Mater.* **2005**, *17*, 2974. (b) Tu, G.; Zhou, Q.; Cheng, Y.; Wang, L.; Ma, D.; Jing, X.; Wang, F. *Appl. Phys. Lett.* **2004**, *85*, 2172. (c) Tu, G.; Mei, C.; Zhou, Q.; Cheng, Y.; Geng, Y.; Wang, L.; Ma, D.; Jing, X.; Wang, F. *Adv. Funct. Mater.* **2006**, *16*, 101. (d) Furuta, P. T.; Deng, L.; Garon, S.; Thompson, M. E.; Fréchet, J. M. J. *J. Am. Chem. Soc.* **2004**, *126*, 15388.
- (20) Nazeeruddin, Md. K.; Humphry-Baker, R.; Berner, D.; Rivier, S.; Zuppiroli, L.; Graetzel, M. *J. Am. Chem. Soc.* **2003**, *125*, 8790.
- (21) (a) Yeh, S.-J.; Wu, M.-F.; Chen, C.-T.; Song, Y.-H.; Chi, Y.; Ho, M.-H.; Hsu, S.-F.; Chen, C.-H. *Adv. Mater.* **2005**, *17*, 285. (b) Li, C.-L.; Su, Y.-J.; Tao, Y.-T.; Chou, P.-Y.; Chien, C.-H.; Cheng, C.-C.; Liu, R.-S. *Adv. Funct. Mater.* **2005**, *15*, 387. (c) Rayabarapu, D. K.; Paulose, B. M. J. S.; Duan, J.-P.; Cheng, C.-H. *Adv. Mater.* **2005**, *17*, 349. (d) Song, Y.-H.; Yeh, S.-J.; Chen, C.-T.; Chi, Y.; Liu, C.-S.; Yu, J.-K.; Hu, Y.-H.; Chou, P.-T.; Peng, S.-M.; Lee, G.-H. *Adv. Funct. Mater.* **2004**, *14*, 1221. (e) Lee, C.-L.; Das, R. R.; Kim, J.-J. *Chem. Mater.* **2004**, *16*, 4642. (f) Nazeeruddin, M. K.; Humphry-Baker, R.; Berner, D.; Rivier, S.; Zuppiroli, L.; Graetzel, M. *J. Am. Chem. Soc.* **2003**, *125*, 8790. (g) Li, H.-C.; Chou, P.-T.; Hu, Y.-H.; Cheng, Y.-M.; Liu, R.-S. *Organometallics* **2005**, *24*, 1329. (h) Justin Thomas, K. R.; Velusamy, M.; Lin, J.-T.; Chien, C.-H.; Tao, Y.-T.; Wen, Y. S.; Hu, Y.-H.; Chou, P.-T. *Inorg. Chem.* **2005**, *44*, 5677. (i) Huang, W.-S.; Lin, J.-T.; Chien, C.-H.; Tao, Y.-T.; Sun, S.-S.; Wen, Y.-S. *Chem. Mater.* **2004**, *16*, 2480. (j) Okada, S.; Okinaka, K.; Iwakaki, H.; Furugori, M.; Hashimoto, M.; Mukaide, T.; Kamatani, J.; Igawa, S.; Tsuboyama, A.; Takiguchi, T.; Ueno, K. *Dalton Trans.* **2005**, 1583. (k) Coppo, P.; Plummer, E. A.; De Cola, L. *Chem. Commun.* **2004**, 1774. (l) Laskar, I. R.; Chen, T.-M. *Chem. Mater.* **2004**, *16*, 111. (m) Kwon, T.-H.; Cho, H. S.; Kim, M. K.; Kim, J.-W.; Kim, J. J.; Lee, K. H.; Park, S. J.; Shin, I.-S.; Kim, H.; Shin, D. M.; Chung, Y. K.; Hong, J.-I. *Organometallics* **2005**, *24*, 1578. (n) Kwong, R. C.; Weaver, M. S.; Lu, M. M.-H.; Tung, Y.-J.; Chwang, A. B.; Zhou, T. X.; Hack, M.; Brown, J. J. *Org. Electron.* **2003**, *4*, 155.

- (22) Kannan, R.; He, G. S.; Yuan, L.; Xu, F.; Prasad, P. N.; Dombroskie, A. G.; Reinhardt, B. A.; Baur, J. W.; Waia, R. A.; Tan, L.-S. *Chem. Mater.* **2001**, *3*, 1896.

- (23) King, K. A.; Spellane, P. J.; Watts, R.-J. *J. Am. Chem. Soc.* **1985**, *107*, 1431.

Scheme 1. Synthetic Route to the Iridium Complex 1



analyses were performed with the Perkin-Elmer Pyris Diamond DSC and Perkin-Elmer TGA6 thermal analyzers. The HOMO and LUMO energy levels of **1** can be estimated from the electrochemical data with reference to the energy level of ferrocene (4.8 eV below the vacuum level) and the first oxidation potentials were used to determine the HOMO energy levels.²⁴

(9,9-Diethyl-7-pyridinylfluorene-2-yl)diphenylamine (HL). (7-Bromo-9,9-diethylfluorene-2-yl)diphenylamine (2.30 g, 4.91 mmol) and 2-(tributylstannyl)pyridine (2.07 g, 5.62 mmol) were mixed in dry toluene (50 mL) and Pd(PPh₃)₄ (0.58 g, 0.50 mmol) was then added to the solution. The resulting mixture was stirred at 110 °C for 24 h. After cooling to room temperature, the reaction mixture was poured into a separating funnel and CH₂Cl₂ (200 mL) was added followed by washing with water (3 × 100 mL). The organic phase was dried over MgSO₄. Solvent was then removed and the residue was purified by column chromatography eluting with CH₂-Cl₂-hexane (3:1, v/v). The ligand HL was obtained as a yellow solid in 79% yield (1.80 g). ¹H NMR (CDCl₃): δ 8.70 (d, *J* = 4.6 Hz, 1H, Ar), 7.98–7.58 (m, 6H, Ar), 7.27–6.97 (m, 13H, Ar), 2.07–1.91 (m, 4H, Et), 0.38 (t, *J* = 7.3 Hz, 6H, Et). ¹³C{¹H} NMR (CDCl₃): δ 157.64, 151.71, 150.31, 149.44, 147.81, 147.30, 142.18, 137.31, 136.49, 135.98, 129.05, 125.81, 123.76, 123.44, 122.42, 121.60, 121.01, 120.54, 120.38, 119.15, 119.13, 56.27, 32.72, 8.71. FAB-MS (*m/z*): 466 [M⁺]. Anal. Calcd. for C₃₄H₃₀N₂: C, 87.52; H, 6.48; N, 6.00. Found: C, 87.25; H, 6.26; N, 5.78. UV-vis (CH₂-Cl₂): λ_{max} (ε × 10⁻⁴M⁻¹cm⁻¹) 301 (1.7), 372 (2.9) nm. PL (CH₂-Cl₂): λ_{em} 446 nm.

[Ir(L)₃] (1). [Ir(acac)₃] (0.15 g, 0.30 mmol) and HL (0.50 g, 1.07 mmol) were combined in glycerol (16 mL). The mixture was heated to 220 °C for 18 h, after which time it was cooled to room temperature and water (50 mL) was added. The resulting mixture was extracted with CH₂Cl₂ (3 × 100 mL) and the organic phase was dried over MgSO₄. After the solvent was removed under vacuum, the residue was purified by column chromatography using CH₂Cl₂ as eluent to afford **1** as an orange solid in 21% yield (0.10 g). ¹H NMR (CDCl₃): δ 7.91 (d, *J* = 8.1 Hz, 3H, Ar), 7.68 (d, *J* = 5.4 Hz, 3H, Ar), 7.58–7.52 (m, 6H, Ar), 7.20–6.77 (m, 45H, Ar), 1.97–1.82 (m, 12H, Ar, Et), 0.45–0.32 (m, 18H, Et). ¹³C{¹H} NMR (CDCl₃): δ 167.00, 160.89, 152.11, 148.11, 147.15, 146.35, 142.91, 142.42, 141.30, 138.15, 135.40, 128.96, 127.79, 123.96, 123.17, 121.83, 121.00, 119.93, 118.81, 118.02, 55.34, 33.58, 32.61, 8.89, 8.63. FAB-MS (*m/z*): 1589 [M⁺]. Anal. Calcd for C₁₀₂H₈₇N₆Ir: C, 77.10; H, 5.52; N, 5.29. Found: C, 76.98; H, 5.33; N, 5.02. UV-vis (CH₂Cl₂): λ_{max} (ε × 10⁻⁴ M⁻¹ cm⁻¹) 309 (7.2), 375 (8.0), 415 (5.5), 478 sh (0.9) nm. PL (CH₂Cl₂): λ_{em} 555, 595 sh nm.

Fabrication of OLEDs and Characterization. Commercial indium tin oxide (ITO) coated glass with sheet resistance of 20–30 Ω was used as the starting substrates. Before device fabrication,

the glass substrate with ~80 nm ITO was first cleaned in deionized water using ultrasonic bath and treated in a UV ozone discharge. The OLED devices were fabricated in a high-vacuum evaporation system under a base pressure less than 2 × 10⁻⁴ Pa without breaking vacuum between each vacuum deposition process. Each of the **1**-doped phosphorescent OLED devices was assembled in the following sequence: ITO on glass substrate (anode), 75 nm of 4,4'-bis[*N*-(1-naphthyl)-*N*-phenylamino]biphenyl (NPB), 20 nm of the emitting layer made of 4,4'-*N,N'*-dicarbazolebiphenyl (CBP) host and phosphorescent dopant (*x*%), 45 nm of 2,2',2''-(1,3,5-phenylene)tris(1-phenyl-1*H*-benzimidazole) (TPBI), 1 nm of LiF, and 60 nm of Al (cathode). The WOLEDs were fabricated in the following configuration: ITO on glass substrate (anode), 60 nm of NPB, 10 nm of the orange-emitting layer made of CBP host and dopant **1** (*x*%), 15 nm of the blue-emitting layer made of *N,N'*-dicarbazolyl-3,5-benzene (mCP) and 8% FIrPic, 40 nm of TPBI, 1 nm of LiF, and 120 nm of Al (cathode). The emissive layer was formed by co-deposition of the dopant and the host in each case. The evaporation rates were 1–2, 0.3, and 4–6 Å s⁻¹ for organic materials, LiF, and aluminum, respectively. The layer thickness was monitored in situ using a quartz crystal oscillator. The active area of the device was 5 mm² as defined by the shadow mask. The electrical and optical characteristics of these devices were measured using R6145 dc voltage current source, FLUKE 45 dual display multimeter, and Spectrascan PR650 spectrophotometer in dark and ambient conditions without packaging.

Results and Discussion

Synthesis and Properties. The synthesis of the diphenylaminofluorene-based iridium cyclometalated complex **1** is outlined in Scheme 1. The cyclometalating ligand HL, which possesses both the hole-transporting diphenylamino moiety

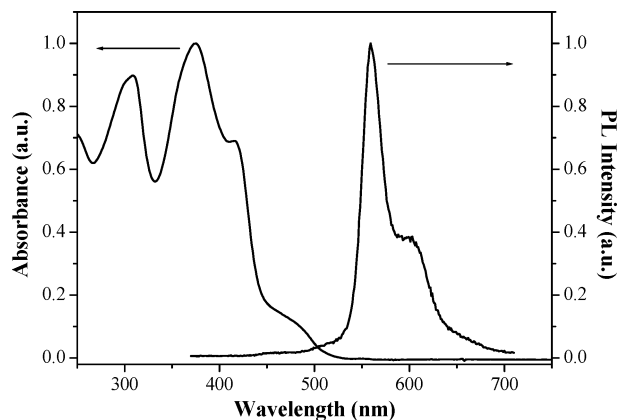


Figure 1. Optical absorption and photoluminescence spectra of **1** in CH₂Cl₂ at 293 K.

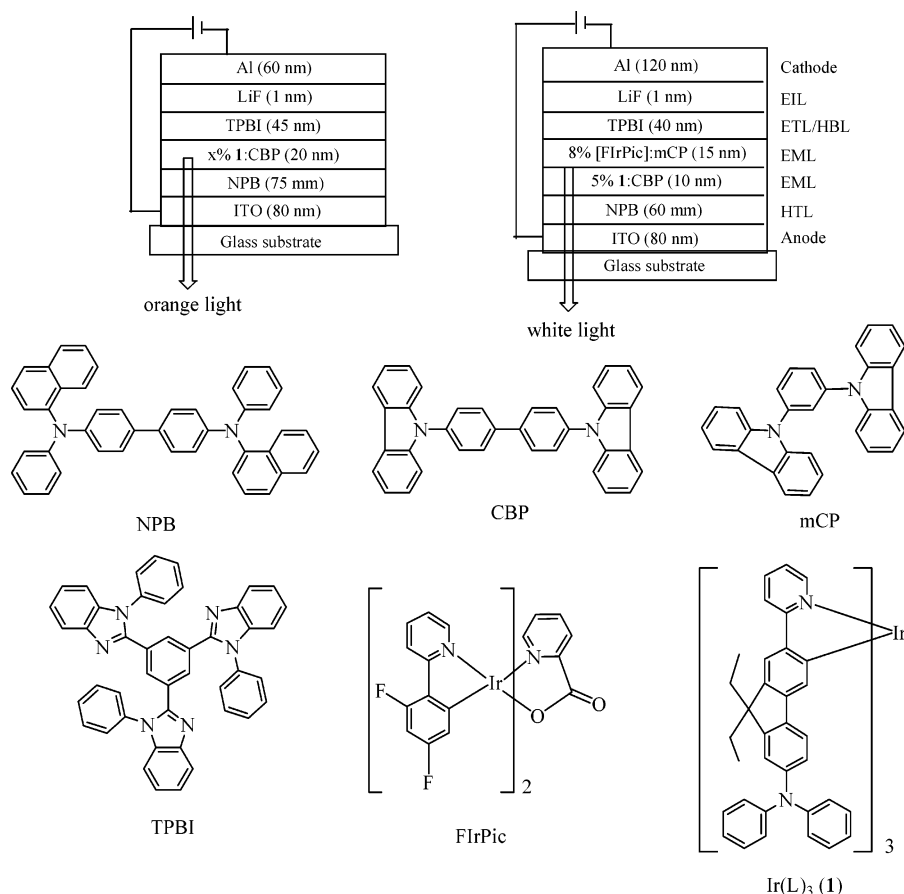


Figure 2. General structures for electrophosphorescent OLED and WOLED devices and the molecular structures of the relevant compounds used in these devices.

and the 2-phenylpyridine cyclometalating site, can be obtained in very good yield from the reaction of (7-bromo-9,9-diethylfluoren-2-yl)diphenylamine²² with 2-(tributylstannyl)pyridine using the Stille coupling synthetic protocol. The homoleptic iridium complex **1** with the formula $[\text{Ir}(\text{L})_3]$ was obtained by the direct thermal reaction of $[\text{Ir}(\text{acac})_3]$ with HL in glycerol under reflux. Purification of the mixture by silica chromatography produced **1** as an air-stable orange powder in high purity and moderate yield (21%). The first-order ^1H and ^{13}C NMR spectra of **1** indicate that the three cyclometalating ligands are magnetically equivalent, in line with a facial geometry around the Ir center.²¹

Complex **1** is a highly amorphous and morphologically stable solid and has a high glass transition temperature (T_g) of 160 °C as revealed by differential scanning calorimetry (DSC). Complex **1** is very thermally stable with decomposition temperature determined by thermogravimetric analysis (TGA) to be 473 °C. In addition, it can be readily sublimed before its decomposition temperature was reached. Because of its very high T_g value, it is less prone to crystallization and such feature is desired for OLEDs of high stability and high efficiency. Relative to the parent complex without the NPh_2 end group which shows a lower T_g value,²⁵ it is clear that the electron-donating NPh_2 unit can help in improving the amorphous nature of the phosphor molecule. We contend that complex **1** will give rise to improved compatibility

between the phosphorescent dopant and the organic host essential for highly efficient electrophosphorescent small-molecule OLEDs.

Figure 1 depicts the optical absorption and photoluminescence (PL) spectra of **1**. Complex **1** is characterized by strong absorption bands at $\lambda_{\text{max}} = 309, 375, 415, 478$ nm. The intense absorptions ($\epsilon \sim 7.2 \times 10^4$ to 8.0×10^4) at $\lambda_{\text{max}} = 309, 375$ nm for **1** resemble those for the free ligand HL ($\lambda_{\text{max}} = 301, 372$ nm) and thus can be assigned to the spin-allowed $^1\pi-\pi^*$ transitions due to the arylamino and amino-fluorenyl segments. Similar spectral assignments have been discussed for related organic molecules by Low and co-workers.²⁶ These $^1\pi-\pi^*$ absorption bands below 400 nm are also accompanied by weaker, lower energy features in the visible regime from 410 to 480 nm that probably correspond to an admixture of $^1\text{MLCT}$, $^3\text{MLCT}$, and $^3\pi-\pi^*$ excited states. The strong spin-orbital coupling between the singlet and triplet manifolds can give rise to the $^3\text{MLCT}$ and $^3\pi-\pi^*$ bands. With reference to previous spectroscopic data for other similar iridium complexes in the literature,²¹ complex **1** emits strong phosphorescence ($\lambda_{\text{em}} = 555$ nm in CH_2Cl_2) from the predominantly ligand-centered $^3\pi-\pi^*$ excited state at the ambient temperature (versus 446 nm for HL). The phosphorescence quantum yield, Φ_p , in degassed

(25) Ostrowski, J. C.; Robinson, M. R.; Heeger, A. J.; Bazan, G. C. *Chem. Commun.* **2002**, 784.

(26) (a) Low, P. J.; Paterson, B. A. J.; Goeta, A. E.; Yufit, D. S.; Howard, J. A. K.; Cherryman, J. C.; Tackley, D. R.; Brown, B. *J. Mater. Chem.* **2004**, *14*, 2516. (b) Low, P. J.; Paterson, M. A.; Puschmann, H.; Goeta, A. E.; Howard, J. A. K.; Lambert, C.; Cherryman, J. C.; Tackley, D. R.; Leeming, S.; Brown, B. *Chem. Eur. J.* **2004**, *10*, 83.

CH_2Cl_2 solution excited at 380 nm is 0.12 for **1**. It shows a phosphorescence lifetime of $\sim 0.08 \mu\text{s}$ in CH_2Cl_2 , shorter than that of the compound without the NPh_2 moiety ($1.2 \mu\text{s}$)²⁷ and most of the reported tris(cyclometalated) iridium complexes.²¹ In the solid state, the lifetime is even shorter ($0.05\text{--}0.08 \mu\text{s}$), presumably due to the phosphorescence self-quenching caused by molecule–molecule interaction.

Our studies show that the incorporation of electron-donating diphenylamino groups to the fluorene skeleton can increase the HOMO level and add the hole-transporting ability to the phosphorescent center. In the cyclic voltammogram, it exhibits two reversible anodic waves at 0.15 and 0.45 V, due to the oxidation of the peripheral arylamino group and Ir-phenyl center, respectively. The reversible reduction occurs primarily on the heterocyclic portion of the cyclometalating ligand at a potential of -1.87 V. Coupling of the NPh_2 group to the fluorene core in **1** lowers the oxidation half-wave potential by ca. 80 mV as compared to the unsubstituted one ($+0.23$ V). Electrochemical data reveal that the HOMO and LUMO levels for **1** were found to be -4.95 and -2.93 eV, respectively. These frontier orbital levels match closely with the energy levels for NPB (HOMO: -5.2 eV) and TPBI (LUMO: -2.9 eV) so that the electronic-structure requirements for the OLED devices can be satisfied. The LUMO level is lower than that of 2-(4-biphenyl)-5-(4-*tert*-butylphenyl)-1,3,4-oxadiazole (PBD, -2.4 eV),²⁸ one of the most widely used hole-blocking/electron-transporting (HB/ET) materials and comparable to that of tris(8-hydroxyquinolino)aluminum (Alq_3 , -3.0 eV). When the NPh_2 terminal groups are anchored to the fluorene rings in **1**, its HOMO value is raised from -5.02 to -4.95 eV relative to the vacuum level. This indicates that complex **1** is more electropositive (or has a lower ionization potential) than the non- NPh_2 capped analogue, leading to a better HT ability in **1**.

Optical and Electronic Characterization of Electrophosphorescent Devices. Figure 2 shows the chemical structures of the materials used in our devices. Complex **1** is sufficiently stable with respect to sublimation for a fabrication process by the vacuum deposition method. In the first set of experiments, simple orange light-emitting devices derived from **1** were studied for the optimization studies. The structure consists of NPB as the hole transport layer (HTL), CBP doped with **1** as the emission layer (EML), TPBI as both the electron transport and hole-blocking layer (ETL/HBL), LiF as the electron injection layer (EIL), and Al as the cathode. Here, TBPI, instead of the commonly used 2,9-dimethyl-4,7-diphenyl-1,10-phenanthroline (BCP) or tris(8-hydroxyquinolino)aluminum (Alq_3), was adopted for the devices to effectively confine excitons within the emissive zone since it has a higher electron mobility and hole-blocking ability.²⁹ To optimize the device efficiency, the thickness

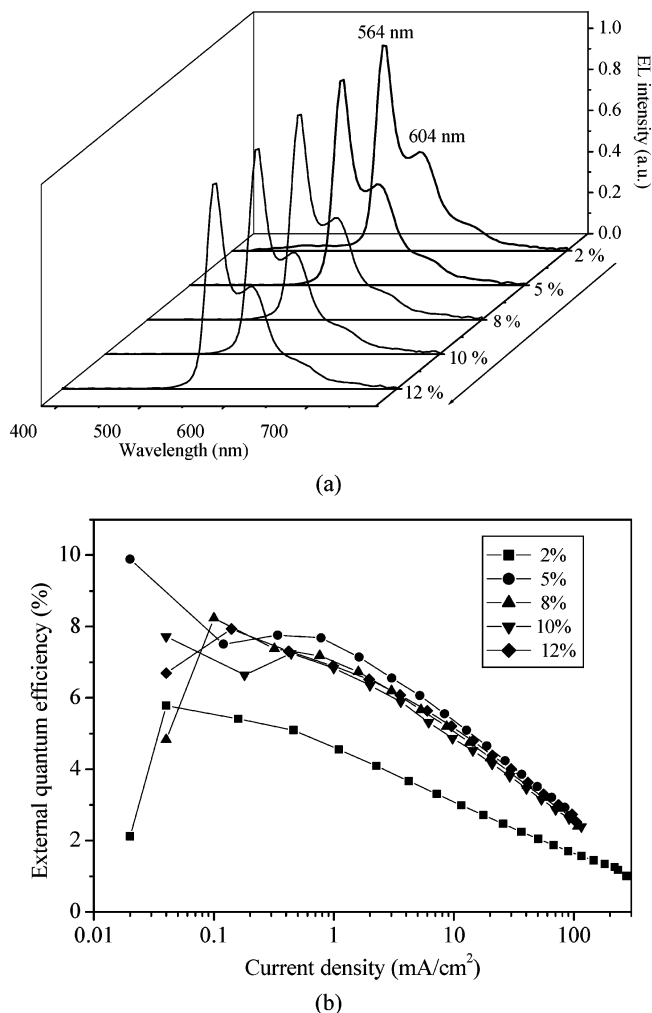


Figure 3. (a) EL spectra and (b) external quantum efficiency versus current density curve of the orange-emitting **1**-doped OLEDs at different dopant concentrations.

of each layer was first fixed (HTL 75 nm, EML 20 nm, and ETL 45 nm), while the doping concentration of **1** was changed from 2 to 12%. The electroluminescence (EL) spectra and external quantum efficiency as a function of current density of these orange-emitting OLEDs are shown in Figure 3a and 3b, respectively. We can see that the major EL peak at 564 nm, with a minor peak around 604 nm, is independent of the dopant level. The device with the 5% doping concentration shows the highest current efficiency of 29.77 cd/A and external quantum efficiency of 9.89% photons/electron, as shown in Figure 3b. The maximum brightness obtained is ~ 8280 cd/m^2 at 12 V. The CIE coordinates of this **1**-doped OLED are (0.50, 0.49), with a color saturation of about 93%. In each case, the EL spectrum resembles its corresponding PL spectrum from thin film, indicating that the same optical transition is responsible for light emission.

Next, with the doping concentration of **1** kept fixed at 5%, the thicknesses of HTL, EML, and ETL were then varied to optimize the OLED devices. It was found that the best performance was obtained for the devices with 55, 25, and 40 nm for the three layers, respectively. Given these considerations, the current–voltage–luminance characteristics and external quantum efficiency versus current density curve of

(27) Tsuboyama, A.; Iwawaki, H.; Furugori, M.; Mukaide, T.; Kamatani, J.; Igawa, S.; Moriyama, T.; Miura, S.; Takiguchi, T.; Okada, S.; Hoshino, M.; Ueno, K. *J. Am. Chem. Soc.* **2003**, *125*, 12971.

(28) Kraft, A.; Grimsdale, A. C.; Holmes, A. B. *Angew. Chem., Int. Ed.* **1998**, *37*, 402.

(29) (a) Wong, K. M.-C.; Zhu, X.; Hung, L.-L.; Zhu, N.; Yam, V. W.-W.; Kwok, H.-S. *Chem. Commun.* **2005**, 2906. (b) Duan, J.-P.; Sun, P.-P.; Cheng, C.-H. *Adv. Mater.* **2003**, *15*, 224. (c) Chen, C. H.; Shi, J.; Tang, C. W. *Macromol. Symp.* **1997**, *125*, 1.

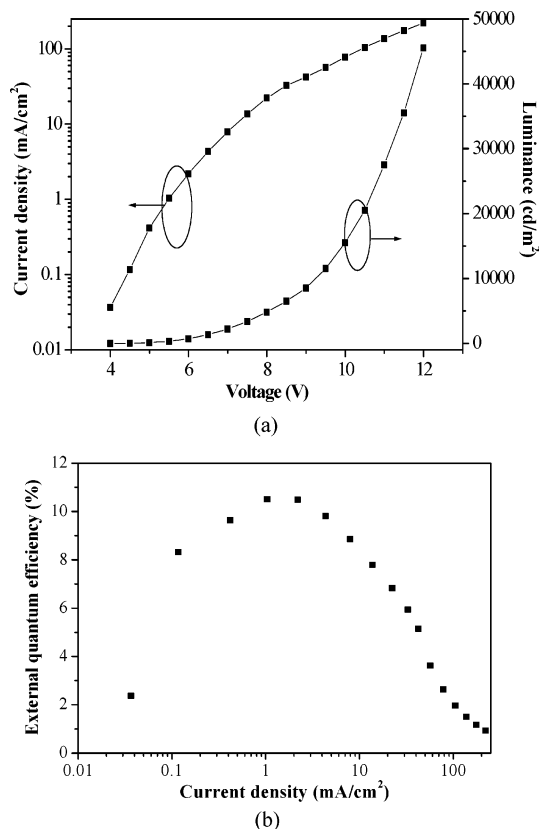


Figure 4. (a) Current–voltage–luminance characteristics and (b) external quantum efficiency versus current density curve in an optimized orange-emitting OLED using 5 wt % of **1**.

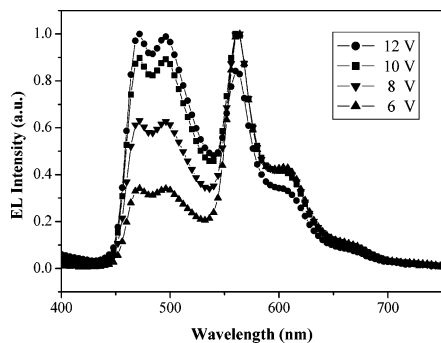


Figure 5. EL spectra of WOLEDs at different voltages.

the optimized device are shown in Figure 4a and 4b. In common with most phosphorescent devices, there was a decrease in efficiency with increasing current density, which has been attributed to a combination of triplet–triplet annihilation³⁰ and field-induced quenching effects.³¹ It was found that a luminance of 4800 cd/m² can be achieved at 8 V (maximum brightness \sim 45530 cd/m² at 12 V) and the highest luminous efficiency attainable is 34.8 cd/A at 1 mA/cm² and 6 V. This corresponds to a peak power efficiency of 18.2 lm/W and an external quantum efficiency of 10.51% photons/electron. This suggests the good potential of using **1** as an orange phosphor dye in fabricating high-efficiency WOLEDs as will be discussed in the following account.

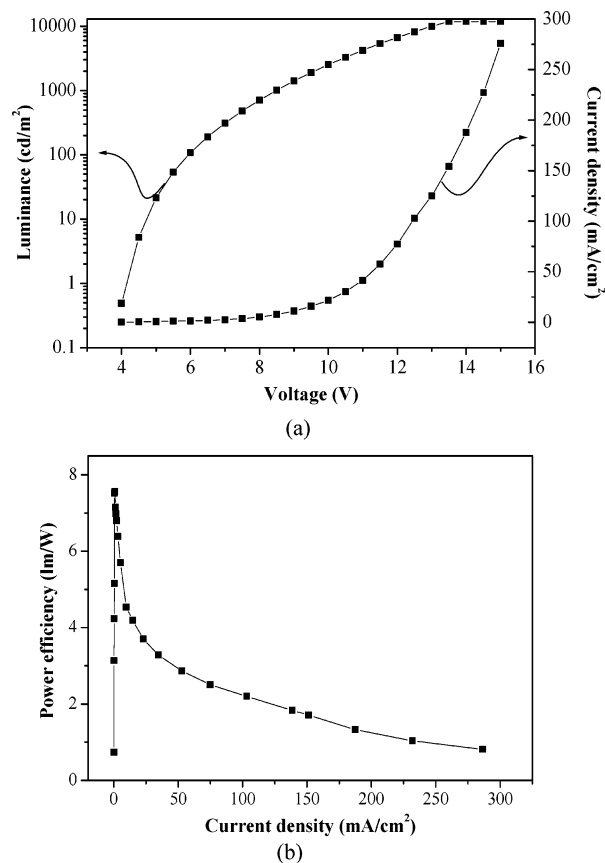


Figure 6. (a) Current–voltage–luminance characteristics and (b) power efficiency versus current density of the electrophosphorescent WOLED device.

The orange color emitted from this device can be suitably coupled with the blue light for color mixing to make multilayered WOLEDs. The WOLED consists of the HTL, EML, and ETL as before. Here, the EML is made up of two independent layers: FlrPic doped in mCP host for the blue light and **1**-doped CBP for the orange light. The layer thicknesses of HTL, ETL, and cathodes were kept to be the same throughout the device fabrication. The effect of the evaporation sequence of the two emission layers was also examined for optimal device results. If the blue-emissive layer was evaporated before the orange-emissive layer, the EL spectrum of the whole device had a much higher peak in the orange region than in the blue region and the CIE white balance was shown to be not good. This means that the energy transfer from mCP to Flrpic is not complete if no hole-blocking layer is deposited next to it. The holes are then easily transported from the blue-emitting layer to the orange-emitting layer. In other words, the recombination process should preferably be completed in the orange-emission layer than in the blue-emission layer. If the evaporation sequence for the EML layers is reversed in order, we could get WOLEDs with satisfactory electrical and optical performance. So it is desirable to deposit the orange-emission layer first, followed by the blue-emission layer in the fabrication process. In such device configuration, an obvious voltage dependence was observed, with the blue emission becoming stronger relative to the orange color at increasing driving voltage, owing to the requirement for high-energy excitation of the blue phosphor. This can also be rationalized

(30) Baldo, M. A.; Adachi, C.; Forrest, S. R. *Phys. Rev. B* **2000**, *62*, 10967.
 (31) Kalinowski, J.; Stampor, W.; Mezyk, J.; Cocchi, M.; Virgili, D.; Fattori, V.; Di Marco, P. *Phys. Rev. B* **2002**, *66*, 235321.

by the fact that the holes have higher mobilities under higher electrical field condition and they will drift to the blue recombination region without being completely recombined in the orange-emitting layer. So the contribution due to the blue light becomes more significant at a higher voltage.⁷

In order to optimize the white light performance, the thickness of each of the two emissive layers was adjusted carefully. It was found that a thickness of 10 and 15 nm for the orange- and blue-emission layer, respectively, provided the best results. The final electrophosphorescent WOLED device structure is shown in Figure 2 and the corresponding EL spectrum is shown in Figure 5. It is clear that when the applied voltage is 10 V, the EL spectrum exhibits two close peaks at 472 and 496 nm, which arise from FIrPic, and a sharp peak at 560 nm due to the orange light emission from the triplet excited state of **1**. The CIE coordinates are located at (0.31, 0.41) at this driving voltage, close to the ideal white point of (0.33, 0.33). Figure 6 depicts the measured current–voltage–luminance profile and power efficiency versus current density curve of this device. The threshold voltage of the WOLED device for light emission at a luminance of 1 cd/m² is about 4.2 V. The luminance reaches 3200 cd/m² at 10 V and 30 mA/cm² with the maximum brightness of 11900 cd/m² being achievable. The peak current and power efficiencies are 17.8 cd/A and 7.6 lm/W, respectively, at $J =$

0.6 mA/cm², which appear to perform better than the device made from the rubrene fluorescent material (~11 cd/A).

Concluding Remarks

In summary, a phosphorescent iridium complex showing high morphological and thermal stability can be exploited to develop orange-emitting OLEDs with the peak electrophosphorescence efficiency reaching 34.8 cd/A at 1 mA/cm² and 6 V. Combination of this metallorganic orange phosphor with another blue phosphor FIrPic in a two-layer EML structure can lead to highly efficient WOLED devices. After optimization of the device structure for the electrical and optical performance, the emission of such WOLED is characterized by the chromaticity coordinates of (0.31, 0.41), a threshold voltage of ~4.2 V, and a maximum brightness of 11900 cd/m². The highest power efficiency could reach 7.6 lm/W at $J = 0.6$ mA/cm², corresponding to a peak luminous efficiency just exceeding 17 cd/A. Work is still underway to improve the color purity and to maximize the device efficiency of these all-phosphor OLED devices.

Acknowledgment. W.-Y.W. thanks the Hong Kong Research Grants Council (Grant No.: HKBU 2022/03P) for the financial support of this work.

CM061030P